Journal of Hydrology 521 (2015) 424–432

Contents lists available at ScienceDirect

Journal of Hydrology

journal homepage: www.elsevier.com/locate/jhydrol

Scaling properties of raindrop size distributions as measured by a dense array of optical disdrometers

Michael L. Larsen *, Timothy B. Hayward [1], Joshua B. Teves

Department of Physics and Astronomy, College of Charleston, SC 29424, USA

ARTICLE INFO

Article history:
Received 22 July 2014
Received in revised form 6 December 2014
Accepted 10 December 2014
Available online 18 December 2014
This manuscript was handled by Andras Bardossy, Editor-in-Chief, with the assistance of Peter F. Rasmussen, Associate Editor

Keywords:
Raindrop size distributions
Scaling
Box-counting fractal dimension
Disdrometer
Power law distribution

SUMMARY

A dense network of optical disdrometers with 1 min resolution was utilized through the winter months of 2013–2014 in South Carolina, USA, to explore the manner in which box-counting fractal dimension is related to drop size. Ten storms of a duration exceeding eight hours were selected for detailed analysis. It was discovered that detector-to-detector variation within each storm was negligible, though storm-to-storm variability could be substantial. The box-counting fractal dimension was found to decrease with increasing drop size, suggesting that large drops are more temporally clustered than small drops. Implications for raindrop sampling are discussed.

1. Introduction

The study of rainfall microstructure has been an active area of research for decades. A central focus for most of this time period has been the study and interpretation of the raindrop size distribution (RSD) (see, e.g., Atlas, 1964; Feingold and Levin, 1986; Jameson and Kostinski, 1998, 2001; Jameson et al., in press; Joss and Gori, 1978; Kostinski and Jameson, 1999; Laws and Parsons, 1943; Marshall and Palmer, 1948; Srivastava, 1971; Ulbrich, 1983, for just a few of the many investigations devoted to RSDs that span the era from the 1940s to the present). The focus on RSDs is principally motivated by the links between the statistical moments of the raindrop size distribution and other variables of physical interest including radar reflectivity, rain rate, liquid water content, drop number density, and drop kinetic energy (see, e.g., Uijlenhoet et al., 2006).

One of the results from the study of rain microstructure is that RSDs often exhibit highly variable behavior over a wide range of temporal and spatial scales (see, e.g., Jaffrain et al., 2011; Jameson and Kostinski, 2000; Jameson et al., in press). Spatial and temporal variability of rainfall and RSDs has impacts on the study of many atmospheric phenomena. To name just a few examples, spatial clustering aloft can influence droplet growth (Kostinski and Shaw, 2005), collision-induced breakup (McFarquhar, 2004), and radiative transmission (Kostinski, 2001).

The spatio-temporal variability of RSDs also presents challenges to the rain investigator seeking to relate point rainfall measurements to extended spatial areas like those utilized in ground validation and/or satellite studies (Tapiador et al., 2012). If point measurements are to be effectively utilized in studies associated with geographically-relevant spatial scales, a more complete quantitative characterization of the natural spatial and temporal variability of rain is necessary (Kostinski et al., 2006).

The detected presence of ground-based RSD temporal variability also has implications for RSD measurement and reporting. In particular, it has been noted that the presence of inhomogeneities in natural rain can influence the interpretation of measured RSDs (Jameson and Kostinski, 2001). This is one primary motivation for efforts to characterize raindrop size-dependent clustering (see, e.g., Kostinski et al., 2006; Larsen et al., 2005; Larsen, 2006; Uijlenhoet et al., 2006). If drops exhibit size-dependent clustering, it is conceivable that an enhanced RSD sampling strategy could be constructed that has some property (e.g. sampling time associated with measurement) that would be raindrop size-dependent as well.

* Corresponding author.
E-mail address: larsenml@cofc.edu (M.L. Larsen).
[1] Present address: Department of Physics, College of William and Mary, Williamsburg, VA 23187, USA.

http://dx.doi.org/10.1016/j.jhydrol.2014.12.016
0022-1694/

Although a variety of different formalisms have been utilized to characterize RSDs (see, e.g., Larsen (2006)), many investigators in the microphysical rain community have recently used scaling (fractal or multifractal) statistical measures (for a small subset of studies utilizing scaling approaches see, e.g., Gupta and Waymire (1990), Larsen et al. (2005), Lavergnat and Golé (1998), Lovejoy and Schertzer (1990), Peters et al. (2002), and Zawadzki (1995)). This approach is very well suited for time-series analysis, has shown recent success in describing temporal rainfall variability in a dense ($\sim$10 m $\times$ 8 m) network of rain gauges (Larsen et al., 2010), and – when using the particularly simple approach of box-counting – enables the investigator to quantify a great deal of information associated with statistical structure into a single numerical parameter (the "box-counting fractal dimension").

In this manuscript, a simple box-counting scaling approach is utilized to examine data from a dense network of optical disdrometers with 1 min temporal resolution. It is shown that there is unambiguous evidence for raindrop size-dependent clustering behavior. The clustering behavior (when characterized with the box-counting fractal dimension) exhibits spatial uniformity over the $\sim$100 m of the array for each studied storm, but storm-to-storm variability can be substantial.

2. Scaling formalism

In the context of atmospheric research, ideas and methods associated with statistical scale invariance have been widely applied. The terminology can refer to an extremely broad range of theoretical structures. The term "fractal dimension" can refer to the Hausdorff dimension, information dimension, correlation dimension, box-counting dimension, or any number of other measures (Peitgen et al., 1992). Additionally, multifractal analysis is rather popular in the hydrological sciences and may ultimately allow deeper insight into the nature of the data. This study constitutes a first step in the investigation of scaling properties of these data via use of the simple-scaling box-counting dimension.

The statistical structure utilized here follows the basic model outlined in Knyazikhin et al. (2005), Larsen et al. (2005), and Zawadzki (1995) and is built around the formula

$$N(\tau) = A\tau^{-f_d}. \quad (1)$$

Here, $N(\tau)$ is the number of disjoint time intervals of duration τ containing at least one "event," A and f_d are fitted statistical parameters, and τ is a time interval that can span from the resolution of the measuring instrument to the total duration of the data set. Within this context, f_d is interpreted as the "fractal dimension" of the data. (The box-counting dimension is used in this study because of its easy implementation, relatively low computational requirements (Fernández-Martínez and Sánchez-Granero, 2012; Foroutan-pour et al., 1999), and to enable comparison to other rain studies (Larsen et al., 2005, 2010; Zawadzki, 1995).)

The reader may have noticed that the term "event" is left ambiguous in the above expression defining f_d. The natural question follows: what quantity is scaling? In Larsen et al. (2005), individual rain drop arrivals (independent of size) were used to define an "event". In Larsen et al. (2010), tipping-bucket rain gauge tip-times (associated with the times total rain accumulation reached an integer multiple of a hundredth of an inch) were used as "events". Both of these studies found some evidence to suggest scaling behavior, but – due to the analysis carried out – neither study was able to directly resolve scaling properties as they were related to RSDs.

Here, an "event" will be construed as the detection of a rain drop by an optical disdrometer in a particular size bin. Thus, a data record from a single disdrometer allows for investigation using the equation

$$N(\tau) = A(D)\tau^{-f_d(D)}, \quad (2)$$

where $N(\tau)$ indicates the number of disjoint time intervals of duration τ containing at least one rain drop associated with some diameter bin D. $A(D)$ and $f_d(D)$ then become fitting parameters that are functions of diameter D.

This study is primarily devoted to exploring the properties and behavior of $f_d(D)$. In particular, the following four questions are investigated. (1) Does $f_d(D)$ vary from detector to detector in a single storm? (2) Does $f_d(D)$ vary from storm to storm? (3) Is $f_d(D)$ related to mean rain rate, number of drops in the storm, storm duration, or peak rainfall intensity? (4) Does the general structure of $f_d(D)$ reveal anything about the drop size distribution and its fluctuations?

3. Experimental setup

To explore the scaling properties of RSDs as described above, data were utilized from a dense array of optical disdrometers located near Hollywood, South Carolina, USA, at 32°44′26″N, 80°10′36″W. This array is located in the South Carolina Lowcountry region, which has a humid subtropical climate (Köppen classification Cfa).

Annual rainfall can vary substantially in this region – a substantial fraction of the annual rainfall can come from tropical storms whose number and intensity vary greatly from year to year – but annual average precipitation is around 130 cm. The array has been constructed on land about 20 km North of the Atlantic coast.

The array of disdrometers includes 21 Thies Laser Precipitation Monitors (hereafter LPMs) (Frasson et al., 2011). The LPMs were deployed in three "arms" as shown in Fig. 1.

This investigation is a small part of another study devoted to understanding rain microphysics on spatial scales smaller than a typical weather radar pixel (see, e.g., Jameson et al., submitted for publication, in press; Larsen et al., 2014; Larsen and Teves, in press). Because of the overarching project goals, the entire disdrometer array has been constructed to fit within a 100 m $\times$ 100 m area, with no two detectors separated by a distance exceeding 125 m.

Each of the LPMs transmits a "data telegram" every minute which reports the number of detected raindrops and assigns each drop to a size and velocity bin. There are 22 non-uniform,

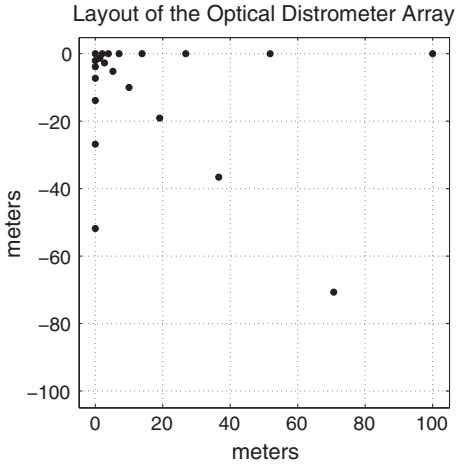

Fig. 1. An illustration of the general layout of LPMs in the instrument array. Each dot indicates the position of a detector. The spacing between detectors is scaled logarithmically to allow for the exploration of multiple spatial scales with a modest number of detectors.

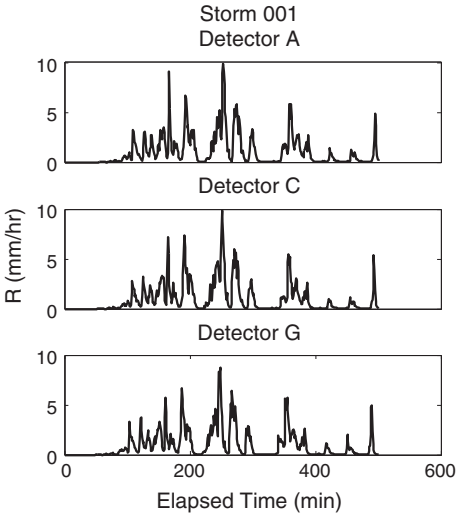

Fig. 2. A plot of the instantaneous (1 min) rain rate as a function of time for three detectors. The storm shown is from 25 March 2014. Agreement between detectors is excellent, though careful examination reveals some differences in the fine details.

non-overlapping size bins and 20 non-uniform, non-overlapping velocities, resulting in 440 total size-velocity combinations. In the data analyzed in this manuscript, the velocity information is discarded and the data from each detector are interpreted as 1-min size spectra with the bin-edges pre-determined by the instrument. All data were recorded by a single data-acquisition computer located approximately 80 m away from the rest of the array.

Data from this array can easily be processed to obtain rain rates, accumulations, and drop size distributions. For example, Fig. 2 demonstrates a plot of rain-rate (1 min resolution) vs. time as detected by three different detectors for one of the storms investigated in more detail below.

The instrument network was constructed during the latter half of 2013 and began acquiring and recording data in late December 2013. More comprehensive descriptions of the instruments used and the array can be found in Frasson et al. (2011), Jameson et al. (in press), and Larsen and Teves (in press).

4. Data and analysis methodology

The ten storms utilized in this study are presented in Table 1. (The word storm is used instead of the more common "rain event" to avoid confusion with the generalized "event" introduced in Section 2.) Storms can be defined using a variety of methods (Ignaccolo and Michele, 2010), but the most common approach is the so-called "minimum inter-event time" method (Dunkerley, 2008). Based on criteria identified from an earlier investigation using this array (Larsen and Teves, in press), a gap of at least one hour preceding and following an interval of rain detection was required for inclusion in this study. Additionally, since identification of scaling relationships require identifying behavior over a wide range of temporal scales (Larsen et al., 2005), only storms with nearly continuous rainfall over an 8+ hour interval were included.

Data used in this manuscript were acquired between late December 2013 and early April 2014. The ten storms studied here have accumulations that add to approximately 22 cm of rainfall. (Typical rain accumulations in the South Carolina Lowcountry annually average approximately 25 cm of rain from January to March.) Thus, even though these 10 events comprise only about 10% of the time interval between late December and early April, a substantial fraction of all winter rainfall accumulations are accounted for by looking at just these ten events.

Depending on the storm in question, either 19, 20, or 21 detectors were utilized for this study. (On some occasions, a detector or two gave unreliable data during a storm; these dubious data records were omitted from the analysis entirely. Summary information for each storm is presented in Table 1.) Although each detector is capable of resolving drop diameters that range from 0.125 mm to 10+ mm, only the first 8 size bins were used in the analysis that follows; these first eight size bins correspond to drop diameters of 0.125–0.250 mm, 0.250–0.375 mm, 0.375–0.500 mm, 0.500–0.750 mm, 0.750–1.000 mm, 1.000–1.250 mm, 1.250–1.500 mm, and 1.500–1.750 mm. (Although only using these first 8 size bins results in missing about 35% of the total detected rain volume, over 98% of all drops are detected in these bins. The sparseness of drops in the bins larger than 1.750 mm renders the numerical method used for the determination of simple-scaling fractal dimension in this manuscript inconclusive.)

In the analysis that follows, the "box-counting method" was implemented (Fernández-Martínez and Sánchez-Granero, 2012): the time series was divided into "boxes" whose durations were characterized by some parameter, τ, and the number of boxes which contain at least one rain drop were counted and assigned to $N(\tau)$. In this way, for large τ we expect $N(\tau) = \tau_{max}/\tau$ (with τ_{max} indicating the duration of the storm) and for small values of τ we must find that $N(\tau)$ equals the number of nonempty minutes for the time series (it is impossible for $N(\tau)$ to exceed this number). On a log–log plot of $N(\tau)$ vs. τ these two regimes exhibit slopes of -1 and 0 respectively (see Fig. 3). Between these two regions, it is possible that there exists an intermediate regime where the trend on the log–log plot is linear with a slope between 0 and -1; the absolute value of this slope was assigned as f_d. Fractal dimensions closer to unity (a time series is inherently one dimensional) correspond to systems with a lesser degree of clustering (see, e.g., Larsen, 2006; Marshak et al., 2005; Shaw et al., 2002). As noted elsewhere (e.g. Larsen et al., 2005), it is possible that there is no linear behavior in the intermediate regime. In these cases, f_d was

Table 1
Storm statistics were averaged over 21 detectors (events 001, 003, 005 and 006), 20 detectors (events 002, 007, 008, 009, 010) or 19 detectors (event 004). Event dates correspond to the first minute of rain data. Accumulations and rain rates were calculated assuming a spherical rain drop and assuming all drops in each bin size corresponded to the smallest possible diameter associated with that bin. Peak rain rate is the mean value of the max 1 min rain rate averaged over all detectors.

Storm	Start time (UTC)	Accum. (mm)	Duration (min)	Mean rain rate (mm/h)	Peak rain rate (mm/h)
001	25 March 2014 03:27	13.1	502	1.6	8.6
002	06 April 2014 14:25	3.9	552	0.5	13.8
003	15 April 2014 13:05	10.8	632	1.0	6.5
004	01 February 2014 12:43	13.1	781	1.0	34.8
005	26 February 2014 12:23	16.4	902	1.1	10.2
006	23 December 2013 19:13	9.4	1052	0.5	14.3
007	07 April 2014 20:25	39.6	1302	2.0	62.5
008	11 February 2014 22:16	44.3	1551	1.8	24.6
009	01 January 2014 11:40	31.3	2302	0.8	6.8
010	16 March 2014 11:54	34.3	3102	0.7	10.7

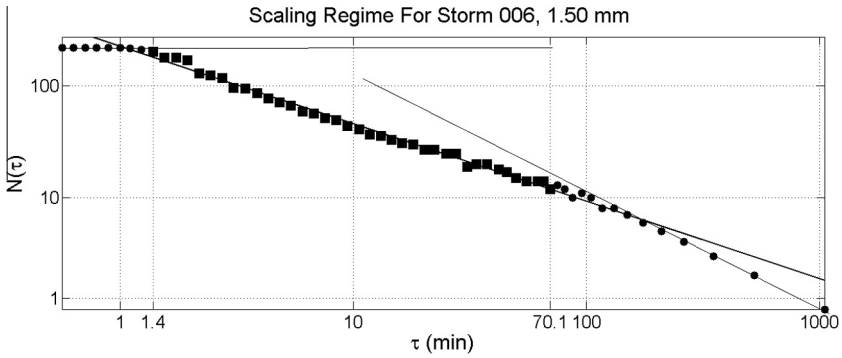

Fig. 3. A plot of $N(\tau)$ vs. τ for the arrival times of drops between 1.50 and 1.75 mm in event 006. In the regime corresponding to box duration between 1.4 min and 70.1 min there is some evidence for fractal scaling behavior (this regime was identified using the algorithms discussed in the appendices). The fit whose slope's absolute value is the fractal dimension of the rain event is plotted over the full figure. The slope in this region is fitted as −0.69. (The 21 detectors detected slopes for this bin during this storm that ranged between −0.722 and −0.664, but we have plotted here the mean of all detectors which gives $f_d = 0.69$.) Additionally, lines of 0 slope, corresponding to the short τ region, and −1 slope, corresponding to the long τ region, are plotted for convenience.

assigned to unity, consistent with systems that do not exhibit scaling behavior (Marshak et al., 2005). More thorough descriptions of the processes used to identify and assign f_d are presented in the appendices.

5. Data analysis

A recent study (using the same array utilized here) has concluded that there is a complex interplay between temporal and spatial fluctuations on scales not typically resolved by weather radar (Jameson et al., in press). At these scales (timescales of minutes and spatial scales of meters), the earlier study concluded that temporal variability and spatial variability may be comparable. In utilizing a different dense network of disdrometers, it was reported that the spatial variability of an RSD over kilometer spatial scales during a single storm can exceed the inter-storm RSD variability (Tapiador et al., 2010). Since the goal in this work was to explore how the scaling parameter f_d depends on various quantities, a natural starting point is to explore the degree to which $f_d(D)$ varies from detector to detector within a single storm. In an effort to quantify the variability of $f_d(D)$ between detectors, the inter-detector variability of $f_d(D)$ is first compared to the inter-storm variability of $f_d(D)$. This methodology is consistent with the general approach taken in Larsen et al. (2010).

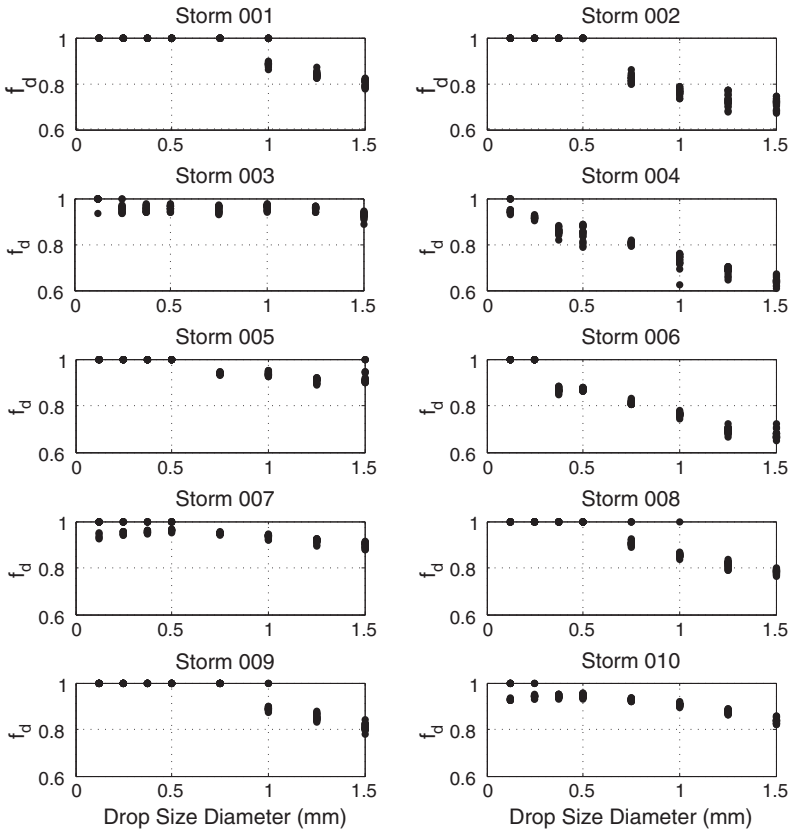

Fig. 4. Fractal dimension as a function of drop size diameter for each of the storms and detectors. Each panel has 19, 20, or 21 data points associated with each drop size (corresponding to the different detectors in the array). Note that in many cases, the variability from detector to detector is imperceptibly small. Throughout this manuscript, graphed drop sizes represent the smallest raindrop size associated with a particular disdrometer size-bin.

5.1. Spatial and inter-event variability of the scaling exponent

In Fig. 4, each panel explores $f_d(D)$ for a particular storm. For each of the first eight size bins, a separate value is shown for each detector. This figure is interesting for multiple reasons. There is clear evidence for limited detector-to-detector fluctuation; each detector is a reasonable estimator of fractal dimension for the entire storm as measured by the entire detector array. This result is somewhat surprising given that other studies which used this same array (e.g., Larsen and Teves, in press), and studies using other arrays (e.g., Tapiador et al., 2010), identified substantial spatial variability of RSDs over the same approximate scales. The consistency of $f_d(D)$ from detector to detector despite the detection of fluctuations using other statistical measures is the first of several results that suggest that the box-counting fractal dimension f_d reveals information distinct from other commonly used statistics associated with RSDs.

Fig. 4 simultaneously reveals that storm to storm variability seems to be substantially larger than spatial variability within a single storm. This likely indicates that knowing a storm's $f_d(D)$ may reveal something about the structure of the storm or, at the very least, can be used as a partial "signature" of the storm. The observation that inter-storm variability exceeds detector to detector variability on small scales is consistent with the results for rain accumulation scaling statistics found in Larsen et al. (2010).

5.2. Fractal dimension as a storm characteristic

Another goal of this study was to identify any links (if they exist) between $f_d(D)$ and other commonly measured or derived storm variables. Consequently, fractal dimension as a function of storm duration, mean rain rate and peak rain rate is plotted for all ten storms in Figs. 5–7. The figures do not reveal an obvious

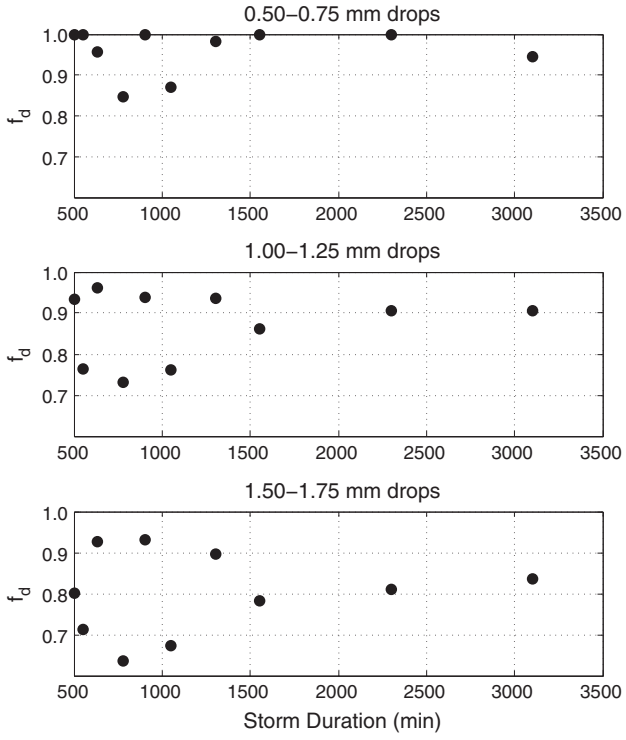

Fig. 5. Fractal dimension as a function of duration of storm for 0.50–0.75, 1.00–1.25, and 1.50–1.75 mm rain drops respectively. Because there is little detector-to-detector variability (see Fig. 4), the mean among all detectors is plotted for each storm. There is no obvious visible correlation between duration of storm and fractal dimension, though the curious behavior for the 8 storms having duration < 2000 min suggest that perhaps further study with more data may reveal new insights.

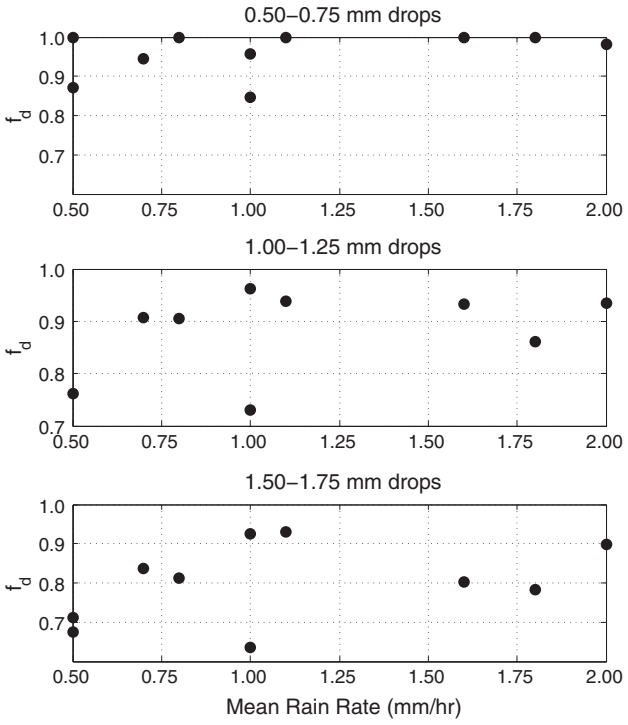

Fig. 6. Fractal dimension as a function of mean rain rate of the storm for 0.50–0.75, 1.00–1.25, and 1.50–1.75 mm rain drops respectively. There is no obvious visible correlation between mean rain rate and fractal dimension.

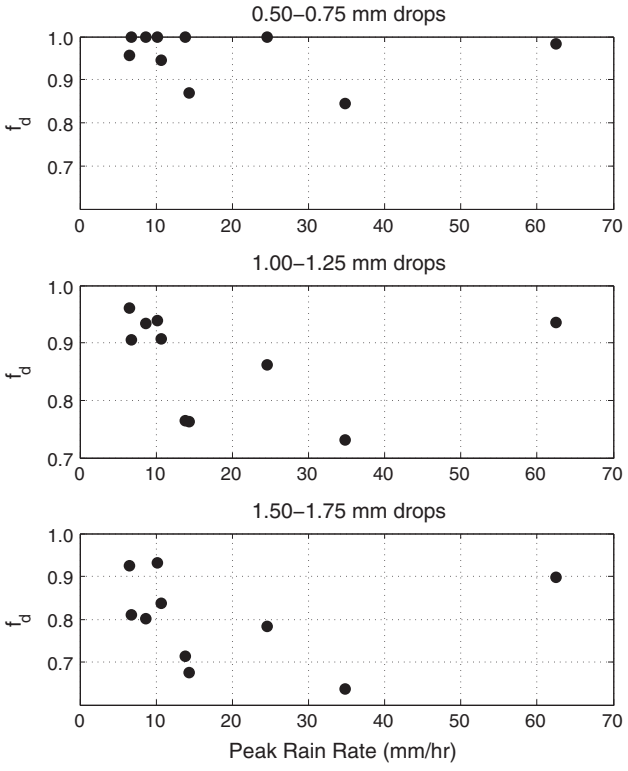

Fig. 7. Fractal dimension as a function of peak rain rate of the storm for 0.50–0.75, 1.00–1.25, and 1.50–1.75 mm rain drops respectively. There is no obvious visible correlation between peak rain rate and fractal dimension.

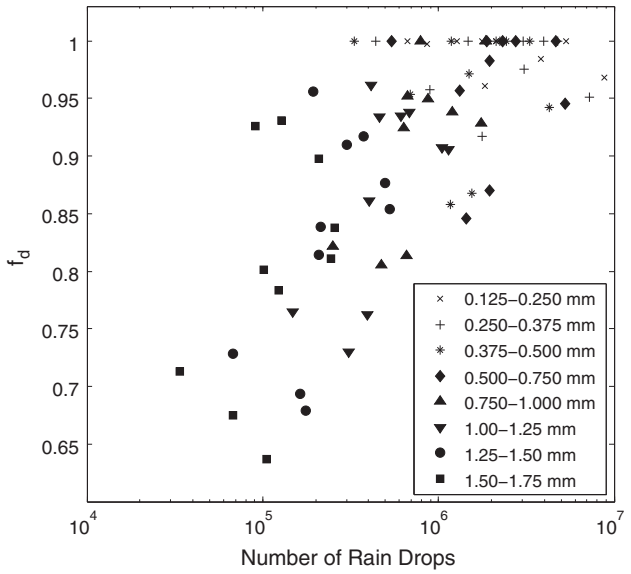

Fig. 8. For each of the smallest 8 size bins associated with each of the 10 storms, the box-counting dimension f_d was calculated. Here, this value of f_d is plotted as a function of the total detected number of drops in the associated time-series (total number of drops detected in the associated size bin for the storm). Each point on the plot represents the average f_d and total number of detected drops among all of the detectors used in the storm (see Table 1). Note that here the ten storms create 80 distinct trials (since each of the first eight size bins constitute an independent measurement for each storm). There is visible evidence for a positive correlation between the box counting fractal dimension and the number of detected rain drops in a data set. Different markers for different size bins reveal the degree to which this trend might actually be linked to drop size instead of drop number. Logarithmic scaling was used on the horizontal axis due to the wide range of drop counts from different sizes.

correlation between these storm properties and fractal dimension, which further suggests that $f_d(D)$ may reveal distinct, new information about the storm.

Fig. 8 reveals a possible link between $f_d(D)$ and the number of drops in a storm. As shown in the figure, data-sets with fewer rain drops tend to be connected with smaller values of f_d. The correlation between these two variables is suggestive, but not conclusive.

One possible explanation of the observed correlation between the number of drops and the value of f_d comes from statistical, rather than physical, considerations. Time series with substantially different numbers of particles but explored over the same time interval will likely have different timescales over which the scaling regime could occur; data sets with fewer(more) particles are more likely to deviate from the -1 regime at larger(smaller) τ. Similarly, data sets with fewer(more) rain drops necessarily reach a smaller(larger) maximum value for $N(\tau)$. These two observations suggest a possible natural bias in the box-counting method toward assigning lower values of f_d to data sets with fewer rain drops. Similarly, as the number of rain drops increases it becomes more and more likely that the storm will appear random at the 1 min resolution. It would be interesting to repeat the same comparison in future studies using instruments with finer temporal resolution.

Another possible explanation of the observed correlation is that the number of observed drops is correlated to some *other* variable that is, in turn, correlated to fractal dimension. In particular, this manuscript considers an explicit dependence of fractal dimension on drop size D. As is well known, RSDs tend to be highly asymmetric with a much larger abundance of drops associated with small sizes (see, e.g., Marshall and Palmer, 1948). As such, the observation that drop number seems to be correlated with scaling parameter f_d may just reflect that drop diameter D is related to scaling parameter f_d. This hypothesis is explored more fully below.

5.3. Drop size distribution

The base motivation for this study was to combine the idea of scale-analysis with the exploration of RSDs. A study of $f_d(D)$ in clouds has revealed a general tendency for larger D to correspond to smaller f_d (Marshak et al., 2005). Studies associated with aerosols have also shown that larger aerosols tend to exhibit a greater degree of particulate clustering than smaller particles (Damit et al., 2014; Larsen et al., 2003; Larsen, 2007). This general trend in behavior (larger D corresponding to smaller f_d) was found to continue here. Throughout all ten storms there is unambiguous evidence for more pronounced scale invariant behavior (clustering) for larger raindrop sizes (recall Fig. 4). Careful examination of Fig. 4 also reveals some general qualitative behavior that varies from storm to storm. In particular:

1. Not all storms exhibited scaling behavior for the same drop sizes. For several storms, no scale invariant behavior was seen for drops less than the fourth size bin (0.50–0.75 mm). Other storms exhibited detectable deviations from $f_d = 1$ for even the smallest (0.125–0.250 mm) size bin.
2. While it is true for all storms that f_d decreases for larger values of D, the scaling parameter f_d can be significantly different for larger drop sizes from storm to storm.

Attempts were made to link quantitative elements of these observations to the physically motivated storm characteristics explored in the previous sections. No obvious connections were identified, though this may be at least in part due to the very limited size of the data set.

Historical rain studies have made extensive use of subdividing populations of storms into different types characterized by RSDs, mean or peak rain rates, or meteorological conditions (Atlas, 1964). This study had a limited ability to discriminate behavior on these characteristics since all data was from the same season and was associated with lengthy, steady, reasonably weak storms likely of the stratiform type. However, a brief analysis of the data available does reveal that the method of subdividing data into

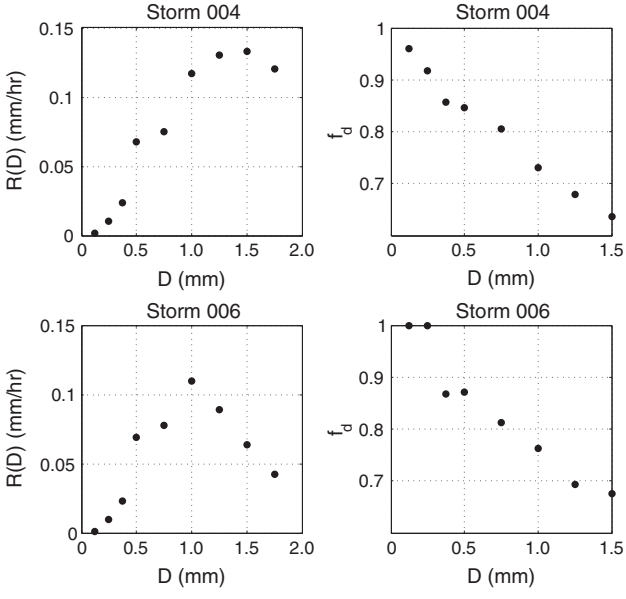

Fig. 9. Mean rain rate contribution (left) and box-counting fractal dimension (right) for different bin sizes for storms 004 and 006. Despite receiving their largest contributions from different bin sizes and having significantly different contributions from large diameter drop sizes, the fractal dimension of both storms behaves almost identically. Recall that the width of each bin size is not the same (see, e.g., Section 3).

meteorological storm-types is likely to be inconclusive. Consider Fig. 9 in which storms 004 (1.0 mm/h mean rain rate and 34.8 mm/h peak rain rate) and 006 (0.5 mm/h mean rain rate and 14.3 mm/h peak rain rate) are pictured. For each of these storms, $f_d(D)$ and the contribution from each drop size to the total mean rain rate are shown. Despite having similar $f_d(D)$, the two storms both receive their largest contribution to rain rate from different drop sizes. Again, a consistent message comes through; it appears that $f_d(D)$ is measuring something different than other commonly reported bulk storm properties. This behavior, which is also found in other storms studied here, has thus far prevented the identification of any quantitative link between $R(D)$ and $f_d(D)$.

Obviously, the different mean RSDs in storms 004 and 006 does not necessarily mean that the storms are meteorologically distinct. Before making any definitive claims about whether $f_d(D)$ behavior can be linked to RSDs, measurements and analysis would need to be completed over multiple seasons to capture a wider variety of storm properties. Future work will hopefully make this clearer.

6. Discussion and conclusions

At the end of Section 2, four specific questions are posed regarding the structure of $f_d(D)$. The analysis above supports the following related conclusions:

1. Analysis of the data unequivocally indicated that $f_d(D)$ does not seem to vary substantially from detector to detector in a single storm on spatial scales up to and including 100 m.
2. Analysis of the data unequivocally indicated that $f_d(D)$ does show storm-to-storm variability.
3. It does not appear that $f_d(D)$ is related to mean rain rate, peak rain rate, or storm duration. There is some suggestive evidence that $f_d(D)$ may be related to number of detected drops, but the evidence is not wholly conclusive at this point.
4. It seems that $f_d(D)$ may reveal some information about RSD structure. More definitive study may be required along these lines, however, to make concrete suggestions.

It should be emphasized that all of the analysis presented here comes from only 10 storms gathered over a time-interval of less than 4 months. These storms were all lengthy (at least 8 h long), but modest in mean intensity. The storms occurred during the least rainy part of the coastal South Carolinian year. As such, there are justifiable reasons to question the degree that the results observed translate to other locations and seasons. Part of the reason for this manuscript is to implore others to conduct similar studies elsewhere; in this way, a more definitive conclusion can be drawn associated with the utility of using $f_d(D)$ to infer RSD properties.

The observation made here that $f_d(D)$ remains uniform across the instrument array for a particular storm is consistent with previous studies (Larsen et al., 2010), yet surprising given the substantial variability seen in the same data using other statistical measures (Jameson et al., in press). This suggests that $f_d(D)$ may be less detector-dependent than other commonly used statistics. Another way to look at this observation, however, is that perhaps $f_d(D)$ is less sensitive to differences than other measures of variability.

The observation that $f_d(D)$ does show storm-to-storm variability suggests that the study of this quantity at least has the potential to lead to insights associated to precipitation microphysics. (If all storms had the same $f_d(D)$ behavior, that would be interesting – but $f_d(D)$ then would not be able to yield any insight into physical processes.)

The observation that $f_d(D)$ appears to be unrelated to mean rain rate, peak rain rate, or storm duration suggests that perhaps $f_d(D)$ does convey some additional information that more traditional rain measures do not directly convey. This may or may not be important, depending on whether or not any microphysical processes can be linked to a measure of $f_d(D)$.

The conclusions associated with specific links between $f_d(D)$ and RSDs are a bit more uncertain at this point. Given that smaller values of f_d are related to a larger degree of clustering, the measurement of $f_d(D)$ for a particular storm may enable a targeted sampling strategy. Systems with larger degrees of clustering are more susceptible to measurement errors associated with insufficient sampling (see, e.g., Larsen and Kostinski, 2009). Thus, if a small value of $f_d(D)$ is observed, perhaps a longer sampling time associated with measurements of drops at the size in question can be associated with a single measurement. This has the potential to reduce uncertainties in the measurement of raindrop sizes that exhibit the most clustering.

The evidence presented here suggests that small values of f_d (for storms in which smaller values of f_d are present) are associated with larger raindrops, consistent with results from both the aerosol particle and cloud drop communities. Consequently, an altered sampling strategy customized to ensure sufficient sampling of large drops could potentially have a substantial impact in disdrometrically inferred values of higher RSD-moment derived quantities like rain rate and radar reflectivity factor.

Acknowledgments

This work was supported by the National Science Foundation (NSF) under Grant AGS-1230240. The authors would also like to thank Michael Chute, Joerael Harris, Robert Lemasters, and Katelyn O'Dell for their work at the array site as well as Arthur Jameson for helpful comments.

Appendix A. Box-counting method

Mandelbrot (1983) discussed a number of methods for estimating the fractal dimension of a system. For this study, the box counting method was chosen because of its easy implementation and relatively low computational requirements (Fernández-Martínez and Sánchez-Granero, 2012; Foroutan-pour et al., 1999). The box-counting method is implemented in this case by dividing the time series into boxes (bins) of successively smaller durations and counting the number of boxes that contain rain. In the case of an infinite system the box-counting fractal dimension would be

$$f_d = \lim_{\tau \to 0} \frac{\log N(\tau)}{\tau}, \tag{3}$$

where τ is some characteristic of the box size in relation to the duration of the data set and $N(\tau)$ is the number of boxes that contain a rain drop. Of course, all real datasets are finite and must be examined over some specific interval. (This is further discussed in Appendix B.)

Let a storm last for total duration τ_{max}. (For each of the storms explored here, $\tau_{max} \geqslant 8$ h.) The largest values of τ examined were τ_{max}/n with n an integer in $[1, 10]$. Between $\tau \sim 1$ min and $\tau_{max}/10$, $\log(\tau)$ were spaced uniformly with 20 different values of τ per decade. This logarithmic spacing for τ is consistent with the basic methodology applied in a wide variety of other scaling studies (e.g., Taouti and Chettih, 2014).

As mentioned in the main text, this method by necessity finds at least two separate linear regimes on the log–log plot of $N(\tau)$ vs. τ due to the finite nature of all datasets. For large values of τ (assuming no substantial "gaps" in the data), $N(\tau) = \tau_{max}/\tau$. At the very least, for $\tau = \tau_{max}$ there must be $N(\tau) = 1$ unless the dataset is null. In the case of the storm systems examined in this work, the next

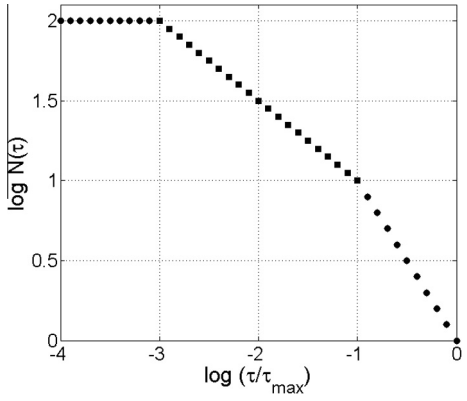

Fig. 10. Idealized behavior for finite fractal data as described in the text. The statistically interesting scaling regime is indicated with boxes.

couple of points should follow this general pattern of $N(\tau_n) = \tau_{\max}/\tau_n$ or else it is likely the length of the storm was misidentified (although, this statement could be complicated somewhat by the fact that larger drops exhibit clumpier behavior). Plotted in double logarithmic space this range of τ values produces a slope of -1.

Similarly, for small values of τ the box-counting method must reach a point in which no further decrease in τ can correspond to an increase in $N(\tau)$. This is because, for a finite system, the algorithm reaches a point in which each data point is occupying its own box. Therefore creating more boxes cannot increase the number of boxes which contain a data point. For data explored in this paper, the instrumental resolution gives a lower bound on τ; no τ less than 1 min is resolvable.

In between these two regimes there may exist a third "transition" regime that could provide evidence for scale invariant behavior. This idea has been discussed at length in Larsen et al. (2010). The absolute value of the slope of this interval is assigned to be the fractal dimension in the box-counting algorithm. An example of an idealized fractal system is pictured in Fig. 10. Real data does not show such clear and well-defined transitions (see, e.g., Fig. 3) and, because of this, some mechanism for identifying the scaling exponent in the transition regime must be applied. As discussed elsewhere there is no universally accepted method for identifying the boundaries of the central scale invariant regime or even an accepted definition for where the regime exists (Larsen et al., 2005). The methodology adopted for this study is outlined in Appendix B.

Appendix B. Fitting algorithm

The fitting algorithm used in this work relies on identifying the two regions which do not exhibit interesting scaling behavior and then discarding them from the fitting process. To identify the first (large τ) regime in which the slope must be approximately -1, a linear best fit was found using the set of the data ranging from τ_i to $\tau_{\max}$ for all values of τ_i identified in Appendix A. The linear fit that corresponded to the longest range of data while also having a slope whose absolute value is greater than a parameter $\alpha = 0.95$ was selected. Similarly, in the small τ limit, a linear best fit was found using the set of the data ranging from $\tau_{\min}$ to τ_j for all values of τ_j identified in Appendix A. The linear fit that corresponded to the longest range of data while also having a slope whose absolute value was less than a parameter $\beta = 0.05$ was selected.

At this point, the two regions identified above were discarded and the remaining data were fit (using a least-squares to the log-transformed data) to a line whose slope's absolute value was assigned as the box-counting fractal dimension of the data set. Finally, it was required that the intermediary region exist over an entire power of ten. (If the identified intermediary region did not exist over an entire power of ten, the data-set in question was identified as "non-fractal" and f_d was assigned to 1.) Thus, data that either did not exhibit any detectable scaling behavior *or* data that exhibited scaling behavior for less than an order of magnitude were mapped to $f_d = 1$.

This method was tested by comparison with the fractal systems outlined in Martínez and Saar (2002) and excellent agreement (accuracy within 5%) was found with theoretical values, with increasing accuracy associated with larger simulated systems. Additionally, the role that α and β played in the fit was examined by adjusting both parameters. Numerical experimentation revealed that adjusting α down to 0.85 and β up to 0.15 changes the inferred value of f_d by at most 10%. Adjustment of numerical fitting parameters did not change any qualitative behavior reported in the main text.

References

Atlas, D., 1964. Advances in radar meteorology. Adv. Geophys. 10, 317–478.

Damit, B., Wu, C., Cheng, M., 2014. On the validity of the Poisson assumption in sampling nanometer-sized aerosols. Aerosol Sci. Technol. 48, 562–570.

Dunkerley, D., 2008. Identifying individual rain events from pluviograph records: a review with analysis of data from an Australian dryland site. Hydrol. Process. 22, 5024–5036.

Feingold, G., Levin, Z., 1986. The lognormal fit to raindrop spectra from frontal convective clouds in Isreal. J. Clim. Appl. Meteorol. 25, 1346–1363.

Fernández-Martínez, M., Sánchez-Granero, M.A., 2012. Fractal dimension for fractal structures: a Hausdorff approach. Topol. Appl. 159, 1825–1837.

Foroutan-pour, K., Dutilleul, P., Smith, D.L., 1999. Advances in the implementation of box-counting method of fractal dimension estimation. Appl. Math. Comput. 105, 195–210.

Frasson, R., da Cunha, L.K., Kra jewski, W.F., 2011. Assessment of the Thies optical disdrometer performance. Atmos. Res. 101, 237–255.

Gupta, V., Waymire, E., 1990. Multiscaling properties of spatial rainfall and river flow distributions. J. Geophys. Res. 98, 1999–2009.

Ignaccolo, M., Michele, C.D., 2010. A point based Eulerian definition of rain event based on statistical properties of inter drop time intervals: an application to Chilbolton data. Adv. Water Resour. 33, 933–941.

Jaffrain, J., Studzinski, A., Berne, A., 2011. A network of disdrometers to quantify the small-scale variability of the raindrop size distribution. Water Resour. Res. 47, W00H006.

Jameson, A., Kostinski, A., 1998. Fluctuation properties of precipitation. Part II: Reconsideration of the meaning and measurement of raindrop size distributions. J. Atmos. Sci. 55, 283–294.

Jameson, A., Kostinski, A., 2000. Fluctuation properties of precipitation. part vi: observations of hyperfine clustering and drop size distribution structures in three-dimensional rain. J. Atmos. Sci. 57, 373–388.

Jameson, A.R., Kostinski, A.B., 2001. What is a raindrop size distribution? Bull. Am. Meteorol. Soc. 82, 1169–1177.

Jameson, A., Larsen, M., Kostinski, A., 2014. On the variability of drop size distributions over areas. J. Atmos. Sci. (submitted for publication).

Jameson, A.R., Larsen, M.L., Kostinski, A.B., 2014. Disdrometer network observations of fine scale spatial/temporal structures in rain. J. Atmos. Sci. (in press).

Joss, J., Gori, E., 1978. Shapes of raindrop size distributions. J. Appl. Meteorol. 17, 1054–1061.

Knyazikhin, Y., Marshak, A., Larsen, M.L., Wiscombe, W.J., Martonchik, J.V., 2005. Small-scale drop size variability: impact on estimation of cloud optical properties. J. Atmos. Sci. 62, 2555–2567.

Kostinski, A., 2001. On the extinction of radiation by a homogeneous but spatially correlated random medium. J. Opt. Soc. Am., A 18, 1929–1933.

Kostinski, A., Jameson, A., 1999. Fluctuation properties of precipitation. Part III: On the ubiquity and emergence of the exponential drop size spectra. J. Atmos. Sci. 56, 111–121.

Kostinski, A., Shaw, R., 2005. Fluctuations and luck in droplet growth by coalescence. Bull. Am. Meteorol. Soc. 86, 235–244.

Kostinski, A.B., Larsen, M., Jameson, A., 2006. The texture of rain: exploring stochastic micro-structure at small scales. J. Hydrol. 328, 38–45.

Larsen, M.L., 2006. Studies of Discrete Fluctuations in Atmospheric Phenomena. PhD Dissertation, Michigan Technological University Department of Physics.

Larsen, M., 2007. Spatial distributions of aerosol particles: investigation of the Poisson assumption. J. Aerosol Sci. 38, 807–822.

Larsen, M., Kostinski, A., 2009. Simple dead-time corrections for discrete time series of non-Poisson data. Meas. Sci. Technol. 20, 095101.

Larsen, M.L., Teves, J.B., 2014. Identifying individual rain events with a dense disdrometer network. Adv. Meteorol. (in press, Article ID 582782).

Larsen, M.L., Cantrell, W., Kannosto, J., Kostinski, A.B., 2003. Detection of spatial correlations among aerosol particles. Aerosol Sci. Technol. 37, 476–485.
Larsen, M.L., Kostinksi, A.B., Tokay, A., 2005. Observations and analysis of uncorrelated rain. J. Atmos. Sci. 62, 4071–4083.
Larsen, M.L., Clark, A., Noffke, M., Saltzgaber, G., Steele, A., 2010. Identifying the scaling properties of rainfall accumulation as measured by a rain gauge network. J. Atmos. Sci. 96, 149–158.
Larsen, M., Kostinski, A., Jameson, A., 2014. Further evidence for super-terminal raindrops. Geophys. Res. Lett. 41, 6914–6918.
Lavergnat, J., Golé, P., 1998. A stochastic raindrop time distribution model. J. Appl. Meteorol. 37, 805–818.
Laws, J., Parsons, D., 1943. The relationship of raindrop size to intensity. Trans. Am. Geophys. Union 24, 452–460.
Lovejoy, S., Schertzer, D., 1990. Fractals, raindrops and resolution dependence of rain measurements. J. Appl. Meteorol. 29, 1167–1170.
Mandelbrot, B.B., 1983. The Fractal Geometry of Nature. W.H. Freeman, New York.
Marshak, A., Knyazikhin, Y., Larsen, M.L., Wiscombe, W.J., 2005. Small-scale drop-size variability: empirical models for drop-size-dependent clustering in clouds. J. Atmos. Sci. 62, 551–558.
Marshall, J.S., Palmer, W.M., 1948. The distribution of raindrops with size. J. Meterol. 5, 165–166.
Martínez, V.J., Saar, E., 2002. Statistics of the Galaxy Distribution. Chapman & Hall, pp. 118–120.
McFarquhar, G., 2004. The effect of raindrop clustering on collision-induced break-up of raindrops. Quart. J. Roy. Meteorol. Soc. 130, 2169–2190.
Peitgen, H.-O., Jürgens, H., Saupe, D., 1992. Chaos and Fractals: New Frontiers of Science. Springer-Verlag, New York.
Peters, O., Hertlein, C., Christensen, K., 2002. A complexity view of rainfall. Phys. Rev. Lett., 88.
Shaw, R.A., Kostinski, A.B., Larsen, M.L., 2002. Towards quantifying droplet clustering in clouds. Quart. J. Roy. Meteorol. Soc. 128, 1043–1057.
Srivastava, R., 1971. Size distribution of raindrops generated by their breakup and coalescence. J. Atmos. Sci. 28, 410–415.
Taouti, M.B., Chettih, M., 2014. Fractal and multifractal analyses of the temporal structure of daily rainfall in a Mediterranean climate in northern Algeria. J. Mediterr. Meteorol. Climatol. 11, 3–12.
Tapiador, F., Checa, R., deCastro, M., 2010. An experiment to measure the spatial variability of rain drop size distribution using sixteen laser disdrometers. Geophys. Res. Lett. 37, L16803.
Tapiador, F.J., Turk, F.J., Peterson, W., Hou, A.Y., Garcia-Ortega, E., Machado, L.A.T., Angelis, C.F., Salio, P., Kidd, C., Huffman, G.J., deCastro, M., 2012. Global precipitation measurement: methods, datasets, and applications. Atmos. Res., 70–97.
Uijlenhoet, R., Porra, J., Sempere-Torres, D., Creutin, J., 2006. Analytical solutions to sampling effects in drop size distribution measurements during stationary rainfall: estimation of bulk rainfall variables. J. Hydrol. 328, 65–82.
Ulbrich, C., 1983. Natural variations in the analytical form of the raindrop size distribution. J. Clim. Appl. Meteorol. 22, 1764–1775.
Zawadzki, I., 1995. Is rain fractal? In: Kundzewicz, Z.W. (Ed.), New Uncertainty Concepts in Hydrology and Water Resources. Cambridge University Press, New York.